Dramatic thermal conductivity reduction by nanostructures for large increase in thermoelectric figure-of-merit of FeSb2

Authors: Huaizhou Zhao, Mani Pokharel, Gaohua Zhu, Shuo Chen, Kevin C. Lukas, Qing Jie, Cyril P. Opeil, Gang Chen, Zhifeng Ren

Dramatic thermal conductivity reduction by nanostructures for large increase in thermoelectric figure-of-merit of FeSb2

Huaizhou Zhao, Mani Pokharel, Gaohua Zhu, Shuo Chen, Kevin Lukas et al.

Additional information on Appl. Phys. Lett.

Dramatic thermal conductivity reduction by nanostructures for large increase in thermoelectric figure-of-merit of FeSb$_2$

Huaizhou Zhao,[1] Mani Pokharel,[1] Gaohua Zhu,[1] Shuo Chen,[1] Kevin Lukas,[1] Qing Jie,[1] Cyril Opeil,[1] Gang Chen,[2] and Zhifeng Ren[1,a)]

[1]*Department of Physics, Boston College, Chestnut Hill, Massachusetts 02467, USA*
[2]*Department of Mechanical Engineering, Massachusetts Institute of Technology, Cambridge, Massachusetts 02139, USA*

In this report, thermal conductivity reduction by more than three orders of magnitude over its single crystal counterpart for the strongly correlated system FeSb$_2$ through a nanostructure approach was presented, leading to a significant increase of thermoelectric figure-of-merit (ZT). For the samples processed with the optimal parameters, the thermal conductivity reached 0.34 Wm^{-1} K^{-1} at 50 K, leading to a ZT peak of about 0.013, compared to 0.005 for single crystal FeSb$_2$, an increase of about 160%. This work suggests that nanostructure method is effective and can be possibly extended to other strongly correlated low temperature thermoelectric materials, paving the way for future cryogenic temperature cooling applications. © *2011 American Institute of Physics*. [doi:10.1063/1.3651757]

Of the several strongly correlated semiconductors including FeSi,[1] Ce$_3$Bi$_4$Pt$_3$,[2] and FeGa$_3$,[3] FeSb$_2$ has recently stimulated extensive research efforts due to its colossal thermopower (Seebeck coefficient, S) at 10 K.[4] The thermopower S of FeSb$_2$ single crystals is on the order of tens of mV K^{-1} which contributes to the very large power factor (PF) of 0.23 Wm^{-1} K^{-2},[4,5] about 40 times of the best thermoelectric materials (Bi$_2$Te$_3$-based high-performance alloy ingots[6,7]). However, it is the figure of merit, $Z = S^2\sigma/\kappa$, where S is the Seebeck coefficient, σ the electrical conductivity, and κ the thermal conductivity, which determines the overall efficiency. To be practically useful, materials should have a dimensionless figure-of-merit (ZT) around 1. However, FeSb$_2$ single crystals have a peak ZT of around 0.005 at 12 K due to a large value of thermal conductivity of about 500 Wm^{-1} K^{-1}.[5] In order for FeSb$_2$ to become a useful material for thermoelectric cooling, ZT must be increased to a meaningful value.

The large lattice thermal conductivity of strongly correlated materials such as FeSb$_2$ at low temperatures limits their ZT. Zhang *et al.*[8] predicted that phonon size effects in nanostructured strongly correlated materials can be exploited to reduce phonon thermal conductivity while maintaining electron transport due to the long phonon mean free path and short electron mean free path. For example, it was estimated that single crystal FeSb$_2$ has an electron mean free path of less than 10 nm at all temperatures with a phonon mean free path around 40 μm at 15 K.[9] This large difference of mean free paths allows the opportunity to tune the electrical and thermal properties almost independently by either doping[10,11] or nano-engineering the grain size.[11] In principle, thermal conductivity suppression can be realized through several different methods such as the introduction of impurities, defects, or grain boundaries. Although substantial thermal conductivity reduction was achieved by doping, no

improvements in ZT were reported due to altered electron transport properties in FeSb$_2$.[10,11]

Nanostructure approach has proven to be a very efficient way to reduce the lattice contribution to the thermal conductivity in many thermoelectric material systems.[12–15] The lower limit of the lattice thermal conductivity in FeSb$_2$ has been calculated[16] to be as low as 0.3 Wm^{-1} K^{-1} at 50 K through the model proposed by Cahill *et al.*[17] It will be shown in this report that the thermal conductivity of nanostructured FeSb$_2$ is drastically decreased leading to an improvement in ZT.

The nanostructured FeSb$_2$ were synthesized by first ingot formation through melting and solidification, and then followed by ball milling and hot pressing with different processing parameters. Scanning electron microscopy (SEM, JEOL 6340F) was used to investigate the grain size distributions of the above processed samples. Transmission electron microscopy (TEM, JEOL 2010F) observation was performed on the representative sample S15hr-200C. The electrical resistivity (ρ), Seebeck Coefficient (S), thermal conductivity (κ), and Hall coefficient (R_H) were all measured on a physical property measurement system (PPMS) from Quantum Design. Within the one-band model, the charge-carrier concentration was determined by $n = 1/(e/R_H/)$. The Hall mobility was determined by $\mu_H = /R_H//\rho$.

SEM images in Fig. 1 show how the grain size changes as a function of ball milling time and hot pressing temperature. From the images, it can be seen that samples pressed from powders ball milled for shorter times (Fig. 1(a)) or at higher temperatures (Fig. 1(d)) have much larger grains than those from powders ball milled for longer time (Figs. 1(b) and 1(c)) and at lower temperatures (Figs. 1(e) and 1(f)). It is also noticed that S15hr-200 C was composed of particles in which there are many smaller grains, which are around 20 ± 5 nm estimated from SEM images (Fig. 1(f)). TEM images shown in Fig. 2 indicate that the particles in sample S15hr-200C were indeed composed of smaller crystalline grains with different orientations, consistent with the SEM image (Fig. 1(f)).

a)Author to whom correspondence should be addressed. Electronic mail: renzh@bc.edu.

An enlarged area from Fig. 2(a) was shown in Fig. 2(b). It is clearly shown that the grains are well-crystallized with dimensions of 20×15 nm and a lattice spacing of 0.276 nm, which can be indexed to the (101) planes of orthorhombic *Pnnm* FeSb$_2$. The nano-sized grains and the boundaries between theses nano-sized crystals would contribute to the dramatic thermal conductivity reductions in the samples.

Figure 3(a) shows the temperature dependence of thermal conductivity for all samples and also the single crystals grown from vapor transport (VT) and self-flux (SF) methods.[5] A substantial decrease of thermal conductivity was found for all samples throughout the temperature range, decreasing as grain size decreases. The thermal conductivity of sample S15hr-600C is 17 Wm^{-1} K^{-1} at 40 K, compared with 0.34 Wm^{-1} K^{-1} for S15hr-200C at the same temperature due to a decrease in the lattice portion of the thermal conductivity. The peak positions of κ, which reveal the competition between the phonon-phonon (Umklapp) scattering or impurity scattering and the grain boundary scattering, shift to higher temperatures and nearly disappear on samples S15hr-200C and S15hr-room temperature. This demonstrates that grain boundary scattering is the dominant scattering mechanism in samples with smaller grain sizes. Moreover, fittings for all the curves below 100 K show a shift from T$^{2.04}$ to T$^{1.31}$ with the decreasing of grain sizes, as is also seen in nanocrystalline silicon[12] which indicates that other parameters besides C_V such as porosity, phonon frequency (ω), and the effective mean free path (Λ_{eff}) also play important roles in thermal conductivity reduction. When compared with single crystal FeSb$_2$, there is a reduction by more than three orders of magnitude in the thermal conductivity from

FIG. 2. TEM images for nanostructured sample S15hr-200C. (a) Lower magnification to show the average grain size and (b) higher magnification of the boxed area shown in (a) to show the crystalline orientation and defected boundaries.

500 Wm^{-1} K^{-1} down to around 0.1 Wm^{-1} K^{-1} at 20 K in the nanostructured sample S15hr-200C. Such a large thermal conductivity suppression by nanostructuring at low temperature is much larger than any other nanostructured thermoelectric materials at high temperatures. Nanostructured *p*-type BiSbTe bulk alloy achieved 83% thermal conductivity reduction compared with its ingot counterpart at 250 °C,[13] half-Heuslers achieved 33% in high temperature ranges,[15] and a 100% reduction for *p*-type silicon germanium alloy.[18]

Figure 3(b) shows the temperature dependence of electrical resistivity for all the samples. The data was fit using Arrhenius' law to find approximate energy gaps. Sample S15hrs-600C has two gaps of 28.2 meV and 4.2 meV. When the pressing temperature is lowered further, e.g., sample S15hrs-300C, only one gap appears with a value of 21 meV. The change in the band gaps corresponds to the increasing of crystal defects that are probably due to the decreased grain size and increased carrier concentration. It appears that the smaller energy gap located in the temperature range of 7-20 K was suppressed; and the larger band gap was decreased as can be seen in the sample pressed at room temperature whose band gap is reduced to 18 meV. Measurements of the carrier concentration, inset of Fig. 3(c) increased as well, confirming the narrowing of the energy gaps.

The temperature dependent Seebeck coefficients (*S*) are shown in Fig. 3(c). It shows that *S* decreases as grain size is decreased, which could mean that carriers are generated. This is not the case for S10min-400C, which has smaller grains than S15hr-600C. From the relationship of the electrical property and the quality of crystal, it is believed that S10min-400C has fewer defects than that of S15hr-600C due to the longer ball milling time of the latter. Defects typically increase carrier concentration, which decreases the *S*. An increase in the carrier concentration will also lead to a decrease in the resistivity, which is the case as seen in Fig. 3(b). Mobility and carrier concentration measurements are shown for two samples in the inset of Fig. 3(c). Carrier concentration at 25 K is higher for the S15hr-300C sample with a value of 9.75×10^{19} cm^{-3} and while its mobility is lower at 4.52 cm^2 V^{-1}s^{-1}, when compared to S15hr-600C at 25 K, whose carrier concentration is decreased to 8.36×10^{17} cm^{-3} while its mobility is as high as 160 cm^2 V^{-1}s^{-1}. These properties directly correlate to the increase seen in the *S*. There is a cross over between the two samples in the Seebeck coefficient found at 65 K. This cross over is also seen in the measurements for carrier concentration at 65 K while the mobility remains relatively constant
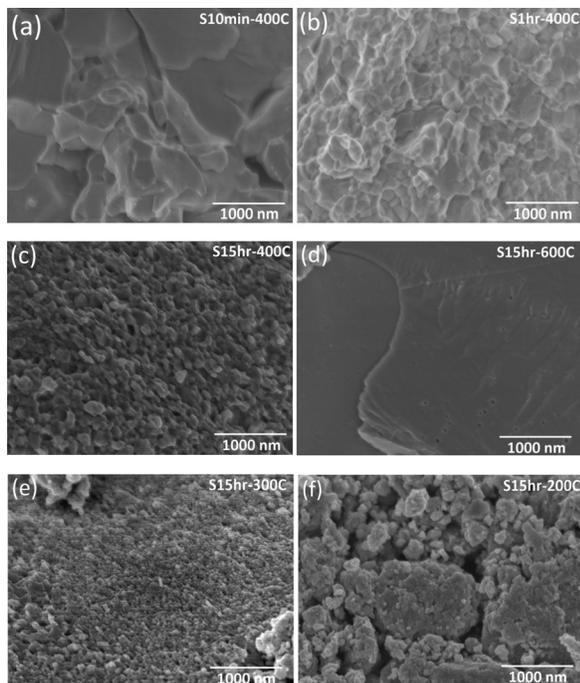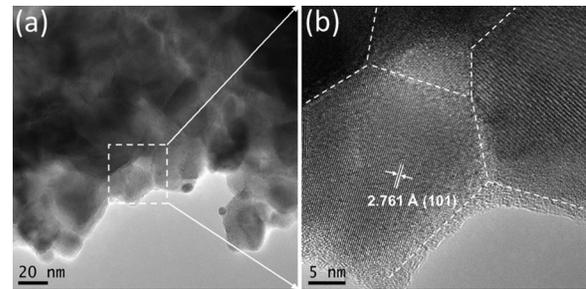

FIG. 1. SEM images for nanostructured samples that were prepared with different conditions. (a) hot pressed at 400 °C using powders ball milled for 10 min, (b) hot pressed at 400 °C using powders ball milled for 1 h, (c) hot pressed at 400 °C using powders ball milled for 15 h, (d) hot pressed at 600 °C using powders ball milled for 15 h, (e) hot pressed at 300 °C using powders ball milled for 15 h, and (f) hot pressed at 200 °C using powders ball milled for 15 h.
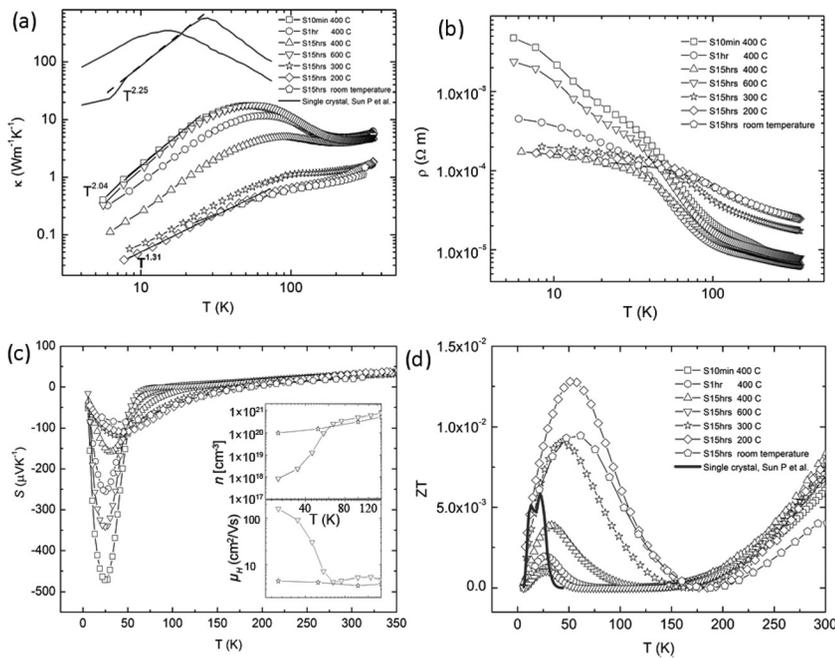
FIG. 3. Thermoelectric properties for nanostructured samples: (a) temperature dependence of thermal conductivity, fittings was applied to sample S10min-400C and S15hr-200C. Two solid curves correspond to thermal conductivity from single crystal samples (Ref. 5); (b) temperature dependence of resistivity; (c) temperature dependence of Seebeck coefficient, the insets indicate the temperature dependent carrier concentration and Hall mobility for S15hr-600C and S15hr-300C, respectively; (d) temperature dependence of ZT.

confirming both measurements. S15hr-600C has better crystallization and therefore a band gap of 4.2 meV in the temperature range 7-20 K, which is not seen in S15hr-300C and induces higher resistivity than that of S15hr-300C below 50 K. For the same reason, peak values of the Seebeck coefficient of S15hr-600C, which is 352 μV K^{-1} at 20 K, is much larger than 117 μV K^{-1} for S15hr-300C at 35 K. In FeSb$_2$ systems, the relation between carrier concentration and Seebeck coefficient has been intensively investigated recently by Sun *et al.*[9,11,19] It was found that an enhancement by a factor of 30 or larger could be applied to the calculated Seebeck coefficient based on the free-electron model. Due to this enhancement, it is quite likely that an increase in the Seebeck coefficient can be realized by tuning carrier concentration through doping or composition adjustment, providing the potential for much future work.

Figure 3(d) shows the temperature dependence of ZT for the nanostructured samples as well as those for single crystals. The ZT increases from 0.001 of sample S15hr-600C to 0.013 of S15hr-200C, which is an unambiguous indication of grain size effect. The optimal ZT value reaching 0.013 at 50 K in S15hr-200C is much higher than $ZT = 0.005$ at 10 K for single crystal samples. Though the power factor is much less than that of single crystal, the drastic reduction in thermal conductivity contributes to the increase in ZT. One feature worth pointing out is that the ZT curve in nanostructured FeSb$_2$ is broadened significantly over that of the single crystal counterpart, which is much more useful for applications between 10 and 150 K.

In conclusion, substantial thermal conductivity suppression for the strongly correlated system FeSb$_2$ through a nanostructure approach was reported in this letter. Thermal conductivity was reduced by more than three orders of magnitude over its single crystal counterpart. As grain size decreases from tens of microns to around 20 nm, the corresponding thermal conductivity decreases by 50 times, reaching 0.34 Wm^{-1} K^{-1} at 50 K. ZT was found to be 0.013, compared to 0.005 for single crystal FeSb$_2$, an increase of 160%. Although this is still far from the state-

of-art requirement of $ZT = 1$, nanostructure to reduce thermal conductivity in FeSb$_2$ is clearly the right way, and a combination with other methods of ZT enhancement including doping or composition adjustment is expected to further increase the ZT.

[1]B. C. Sales, E. C. Jones, B. C. Chakoumakos, J. A. Fernandez-Baca, H. E. Harmon, J. W. Sharp, and E. H Volckmann, Phys. Rev. B: Condens. Matter. **50**(12), 8207 (1994).

[2]M. F. Hundley, P. C. Canfield, J. D. Thompson, and Z. Fisk, Phys. Rev. B **50**(24), 18142 (1994).

[3]Y. Hadano, S. Narazu, M. A. Avila, T. Onimaru, and T. Takabatake, J. Phys. Soc. Jpn. **78**(1), 013702 (2009).

[4]A. Bentien, S. Johnsen, G. K. H. Madsen, B. B. Iversen, and F. Steglich, Europhys. Lett. **80**, 17008 (2007).

[5]P. Sun, N. Oeschler, S. Johnsen, B. B. Iversen, and F. Steglich, J. Phys.: Conf. Ser. **150**, 012049 (2009).

[6]O. Yamashita, S. Tomiyoshi, and K. Makita, J. Appl. Phys. **93**, 368 (2003).

[7]S. Paschen, in *Thermoelectric Handbook*, edited by D. M. Rowe (CRC Press, Taylor & Francis Group, Boca Raton, 2006), Chap. 15.

[8]Y. Q. Zhang, M. S. Dresselhaus, Y. Shi, Z. F. Ren, and G. Chen, Nano Lett. **11**(3), 1166 (2011).

[9]P. Sun, N. Oeschler, S. Johnsen, B. B. Iversen, and F. Steglich, Phys. Rev. B **79**(15), 153308 (2009).

[10]A. Bentien, G. K. H. Madsen, S. Johnson, and B. B. Iversen, Phys. Rev. B **74**(20), 205105 (2006).

[11]P. Sun, M. Søndergaard, Y. Sun, S. Johnsen, B. B. Iversen, and F. Steglich, Appl. Phys. Lett. **98**, 072105 (2011).

[12]Z. Wang, J. E. Alaniz, W. Jang, J. E. Garay, and C. Dames, Nano Lett. **11**(6), 2206 (2011).

[13]B. Poudel, Q. Hao, Y. Ma, Y. Lan, A. Minnich, B. Yu, X. Yan, D. Wang, A. Muto, D. Vashaee, X. Chen, J. Liu, M. S. Dresselhaus, G. Chen, and Z. F. Ren, Science **320**(5876), 634 (2008).

[14]Y. C. Lan, A. J. Minnich, G. Chen, and Z. F. Ren, Adv. Funct. Mater. **20**, 357 (2010).

[15]X. Yan, G. Joshi, W. S. Liu, Y. C. Lan, H. Wang, S. Lee, J. W. Simonson, S. J. Poon, T. M. Tritt, G. Chen, and Z. F. Ren, Nano Lett. **11**, 556 (2011).

[16]S. Zhu, W. Xie, D. Thompson, T. Holgate, M. Zhou, Y. Yan, and T. M. Tritt, J. Mater. Res. **26**(15), 1894 (2011).

[17]D. G. Cahill, S. K. Watson, and R. O. Pohl, Phys. Rev. B **46**(10), 6131 (1992).

[18]G. Joshi, H. Lee, Y. Lan, X. Wang, G. Zhu, D. Wang, R. W. Gould, D. C. Cuff, M. Y. Tang, M. S. Dresselhaus, G. Chen, and Z. F. Ren, Nano Lett. **8**(12), 4670 (2008).

[19]P. Sun, N. Oeschler, S. Johnsen, B. B. Iversen, and F. Steglich, Dalton Trans. **39**, 1012 (2010).